



## Thermal modeling of the respiratory turbinates in arctic and subtropical seals

Eirik G. Flekkøy<sup>a,\*</sup>, Lars P. Folkow<sup>b</sup>, Signe Kjelstrup<sup>a</sup>, Matthew J. Mason<sup>c</sup>, Øivind Wilhelmsen<sup>a</sup>

<sup>a</sup> PoreLab, Department of Chemistry, Norwegian University of Science and Technology, NTNU, Trondheim, Norway

<sup>b</sup> Department of Arctic and Marine Biology, University of Tromsø - the Arctic University of Norway, Norway

<sup>c</sup> Department of Physiology, Development & Neuroscience, University of Cambridge, Cambridge, UK

### ARTICLE INFO

#### Keywords:

Respiratory turbinate  
Water conservation  
Body heat conservation  
Arctic seal  
Thermoregulation  
Homeotherm

### ABSTRACT

Mammals possess complex structures in their nasal cavities known as respiratory turbinate bones, which help the animal to conserve body heat and water during respiratory gas exchange. We considered the function of the maxilloturbinates of two species of seals, one arctic (*Erignathus barbatus*), one subtropical (*Monachus monachus*). By means of a thermo-hydrodynamic model that describes the heat and water exchange in the turbinate region we are able to reproduce the measured values of expired air temperatures in grey seals (*Halichoerus grypus*), a species for which experimental data are available. At the lowest environmental temperatures, however, this is only possible in the arctic seal, and only if we allow for the possibility of ice forming on the outermost turbinate region. At the same time the model predicts that for the arctic seals, the inhaled air is brought to deep body temperature and humidity conditions in passing the maxilloturbinates. The modeling shows that heat and water conservation go together in the sense that one effect implies the other, and that the conservation is most efficient and most flexible in the typical environment of both species. By controlling the blood flow through the turbinates the arctic seal is able to vary the heat and water conservation substantially at its average habitat temperatures, but not at temperatures around  $-40^{\circ}\text{C}$ . The subtropical species has simpler maxilloturbinates, and our model predicts that it is unable to bring inhaled air to deep body conditions, even in its natural environment, without some congestion of the vascular mucosa covering the maxilloturbinates. Physiological control of both blood flow rate and mucosal congestion is expected to have profound effects on the heat exchange function of the maxilloturbinates in seals.

### 1. Introduction

Survival in different environments has required animals to evolve mechanisms that enable them to maintain homeostasis under a range of often challenging conditions. In air-breathing vertebrates, the necessary and life-sustaining process of lung ventilation potentially challenges their water balance and, in homeotherms, the thermal balance. This is because the gas mixture within the lungs is warmed to body temperature and saturated with water vapor, and if no steps were taken the added heat and water would simply be lost on expiration. Strategies to reduce heat loss via breathing may be important compared to other heat conserving strategies, such as insulation or adaptation of the surface to volume ratio of the animal (Favilla and Costa, 2020).

In mammals, the nasal cavity is involved in the conditioning of the inhaled and exhaled gases, e.g. Walker et al. (1961). Projecting into the

nasal cavity of mammals are the turbinate bones. These are thin, scroll-like or dendritic in structure, and lined with olfactory or respiratory epithelia. Efficient exchange of heat and water is secured by the functional subdivision of these bones known as respiratory turbinates, of which the maxilloturbinates (MT) form by far the largest part e.g. (Negus, 1958; van Valkenburgh et al., 2011; Mason et al., 2020). The MT exposes a large surface area of richly vascularized nasal mucosa (MT surface area, from now on denoted MSA) to the respiratory air-stream, e.g. (Folkow et al., 1988). These structures have been shown to serve an important heat and water conserving function in a process called nasal temporal counter-current heat exchange, or simply nasal heat exchange (Walker et al., 1961; Schmidt-Nielsen et al., 1970; Blix and Johnsen, 1983).

On inhalation of cold air, heat flows from the MSA to the incoming air and the air temperature increases towards deep body temperature.

\* Corresponding author.

E-mail address: [flekkoy@fys.uio.no](mailto:flekkoy@fys.uio.no) (E.G. Flekkøy).

<https://doi.org/10.1016/j.jtherbio.2022.103402>

Received 30 May 2022; Received in revised form 21 November 2022; Accepted 22 November 2022

Available online 6 January 2023

0306-4565/© 2023 The Authors. Published by Elsevier Ltd. This is an open access article under the CC BY license (<http://creativecommons.org/licenses/by/4.0/>).

Simultaneously, water will evaporate from the moist MSA until saturation of the inspired air. On exhalation, the respiratory gases are cooled on encounter with the cold MSA upon which water vapor condenses, thereby allowing recovery of heat and water, including the latent heat of condensation. Any deficit in the balance of the two parts of the cycle must be supplied from the blood stream.

Phocid seals possess particularly complex MT (Negus, 1958; Folkow et al., 1988; Mason et al., 2020; Huntley et al., 1984). Their elaborate maxilloturbinates (MT) are positioned in the nasal cavity, rostral to the olfactory region (OT), see Fig. 2. Based on computed tomography scans, Mason and coworkers (Mason et al., 2020) recently described the morphology of the MT in 8 species of seals, including measurements of the total MSA. The dendritic maxilloturbinates were found to be considerably more elaborate in polar species (Fig. 1B) than in subtropical species (Fig. 1A). Polar species had greater total MSAs, greater nasal cavity cross-sectional areas and narrower channel widths between their maxilloturbinate bones.

Functionally, during ventilation through the MT, air will flow through multiple, parallel, fine-caliber passages of length  $L$  (Fig. 2), while a perpendicular section through the structure (Fig. 1) reveals a branching or labyrinthine construction of channels of width  $w$  that fill the nasal cavity.

Here, we seek to understand the function and physiological flexibility of the maxilloturbinates from a physical model. This model relies on a simplified description of the coupled thermodynamics and hydrodynamics of a single channel through the turbinates: as inhaled air flows along this channel, heat and vapor diffuses across the streamlines of the flow so as to deliver both heat and humidity to the air. This is described by the mathematical model which takes measured lengths and widths of the channels through the turbinates as input and delivers both tissue and air temperature profiles along the channel as a result. The model includes the effect of a variable heat supply from the blood. The minimum blood velocity is set in order to fulfill the condition that it keeps the outer parts of the turbinates from freezing, while the maximum is set from consideration of the flow capacity of the arterial vessels. Apart from confirming that the turbinate design is in fact well suited (1) to equilibrate the air at the relevant environmental conditions, and (2) to conserve heat and water, the model is used to explore variations in the physiological parameters not easily controlled in experiments or measured experimentally. In particular, it makes it possible to explore how the animals adapt to variations in the environmental conditions by means of changing the arterial blood flow.

Similar models have been made of other species. Magnanelli et al. (2017) and Solberg et al. (2020) modeled a recovery of water and heat near 90% in the nasal cavity of reindeer, given a supply of energy from a blood flow of moderate/low velocity.

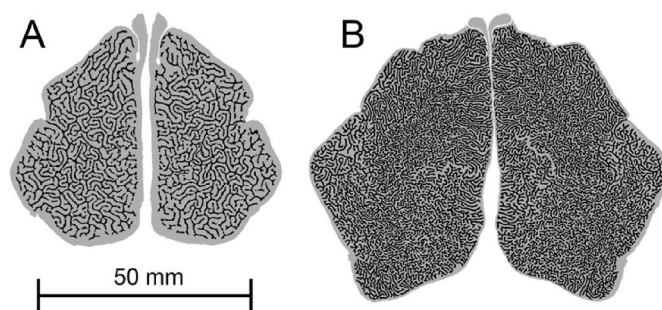


**Fig. 1.** The structure of the maxilloturbinates of A) a subtropical seal (*Monachus monachus*), and B) an arctic (*Erignathus barbatus*) obtained by micro-computed tomography (micro-CT) sections through the maxilloturbinate region. The figure shows a cross section in the plane perpendicular to the air flow through the maxilloturbinates of each seal. The air pathways are shown in grey, the maxilloturbinates in black. The image is reproduced with permission from Mason et al. (Mason et al., 2020).

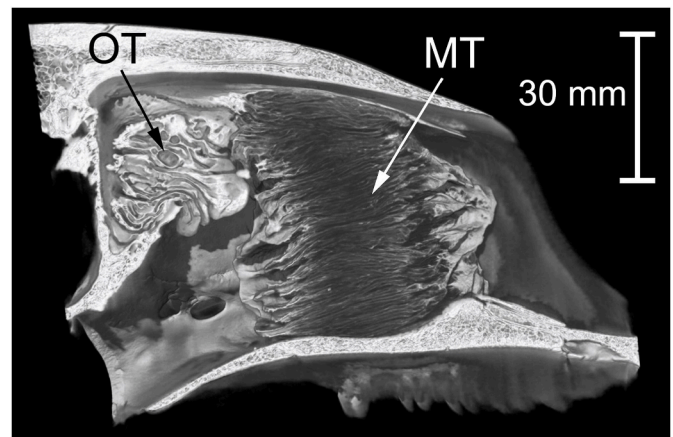


**Fig. 2.** Reconstruction of the left turbinate structures of *Erignathus barbatus*, obtained from micro-CT scans. The figure shows a sagittal section through the nasal cavity in a plane along the airflow; anterior is to the right. The olfactory turbinates (OT) and maxilloturbinates (MT) are indicated. The image is reproduced with permission from Mason et al. (Mason et al., 2020).

Based on latitudinal differences in MT-complexity between seal species, Mason and coworkers argued (Mason et al., 2020) that heat conservation is likely the main driver for the observed differences between seals. This is supported by the fact that heat/water exchange efficiency in seals is subject to thermoregulatory control (Folkow and Blix, 1989), but apparently not to osmoregulatory control (Skog and Folkow, 1994). However, the conservation of heat implies corresponding conservation of water, that is, the two processes go hand-in-hand in the phase transition of water.

The aim of this work is to add to the analysis of Mason et al. (2020) using the model simulations to find the impact of ambient conditions on the evolution of seal MTs. The model describes the local exchange of thermal energy along the MT. We shall find that for both species the model explains the turbinate design (length scales) while suggesting the possibility of flexible control of heat and water release under typical environmental conditions.

The paper is organized as follows. In section 2 we introduce and discuss the physiological measurements. In section 3 we introduce the physical model. The model includes the effects of a variable blood supply and the effect of ice forming in the outer turbinate parts. In section 4 the model is applied to obtain temperature profiles and their variation with ambient air temperature, breath duration and tidal volume. These results are finally interpreted in section 5.

## 2. Materials and methods

### 2.1. Two seals and their ambient conditions

As a representative of arctic seals we have chosen the bearded seal (*Erignathus barbatus*, abbreviated Eb from now on), while the monk seal (*Monachus monachus*, abbreviated Mm) was chosen to represent warm-water seals. Anatomical data from two Mm specimens were averaged. Physiological data are not abundant for these seals, and some values we use are therefore taken from the grey seal (*Halichoerus grypus*) (Reed et al., 1994; Folkow and Blix, 1987).

The average body mass (BM) of the grey seals, from which important physiological data were obtained (Reed et al., 1994), is 180 kg, which is within the range of normal BM for both Eb and Mm (Kenyon, 1981; Burns, 1981), and they can be assumed to have the same total lung capacity of 14.6 l (Kooymann, 1989). Rather than the total lung capacity, however, we consider the tidal volume as more relevant for the analysis of respiration. The tidal volume listed in Table 1 represents the mean air volume shifted through the nasal cavity during each exhalation, in four

**Table 1**  
Physiological data.

Property	Symbol	Species Eb	Mm	Reference, Comment
Tidal lung volume	$V_t/l$	6.3	6.3	Resting in water (Reed et al., 1994)
Time of inhalation	$t_{br}/s$	1.1	1.1	Reed et al. (1994)
Mean MT length	$L_{MT}/cm$	2.5	2.0	Appendix A.1
Total cross-sectional area	$A/cm^2$	36.5	18.6	Appendix A.1
Cross-sectional area air	$A_a/cm^2$	20.3	12.7	Appendix A.1
MT tissue width	$w_t/mm$	0.27	0.31	Appendix A.1.
MT channel width	$w/mm$	0.34	0.65	Appendix A.1
Mean flow velocity	$u/(m/s)$	2.3	4.0	

180 kg grey seals while resting between dives in water (Reed et al., 1994).

Micro-CT images created by Mason et al. (2020) were used to find good estimates for the anatomical variables. The CT scans were made of prepared skulls, but there may have been dried soft tissue clinging to the turbinate bones within the nasal cavity which could not be distinguished from the bone itself. By comparison with a photomicrograph of the grey seal turbinate region presented in (Folkow et al., 1988), the widths of the maxilloturbinates shown in the processed scans (e.g. Fig. 1) appeared sufficient to include a vascularized mucosal layer covering the bone. The detailed procedures for making anatomical measurements from these scans can be found in Appendix A.1 and Appendix B, while results are listed in Table 1. The geometric characteristics such as channel widths are given in Table 1.

For simplicity  $T_b$  was assumed to be 35 °C for both seals (Folkow and Blix, 1987). Average ambient conditions for these seals were estimated using data from various sources [9, 14, 15, 16, 17], see Appendix B for details. The annual global temperature map was used for ambient temperatures (Matsuura, 2020).

The data of Table 2 and 3 are needed for the modeling. By adopting them we immediately see a large variation between the different locations on earth. For the arctic and sub-tropical seals we obtain the average values  $T_b - T_a = 40$  (15)°C for Eb (Mm). The amount of water needed for saturation of the inhaled air, under reasonable assumptions of climatic conditions in their respective habitats, was estimated to be 0.231 g (Eb) and 0.16 g (Mm), see Appendix A.1.

### 3. Model for the heat and water exchange in the turbinate

The model is based on the geometry shown in Fig. 3. Clearly, time is needed for diffusive transport of heat and vapor between the air in the channel and its wall, an exchange that takes place over a limited length,  $L$ , of the turbinate. For water molecules in the air to condense on exhalation, there must be sufficient time for the molecule to travel from the channel center to the nearest wall by diffusion, and the same is true for the heat. If the channel is too wide, only the humidity and thermal energy contained in a boundary layer will reach the wall. The critical distance is thus the channel half width. In reality, there are no single channels. The cross-section made perpendicular to the flow (Fig. 1), shows a labyrinthine, inter-connected pattern. In our simplified model we shall nevertheless model the MT organ as composed of a bundle of

**Table 2**  
Estimated average temperatures for arctic and subtropical seals.

Property	Symbol	Species Eb	Mm	
Ambient air temperature	$T_a/°C$	-5	20	[16, 17, 19]
Deep body temperature	$T_b/°C$	35	35	Folkow and Blix (1987)

**Table 3**  
Physical chemical data taken from (Aylward and Findlay, 2002).

Property	Symbol	Dimension	Value
Density, water	$\rho_w$	kg/m <sup>3</sup>	10 <sup>3</sup>
Heat of evaporation, water	$\Delta H$	J/kg	2.5 10 <sup>6</sup>
Specific heat capacity, tissue	$c_w$	J/(K kg)	3480
Specific heat capacity, air (at 1 bar)	$c_a$	kJ/(m <sup>3</sup> K)	1.24
Heat capacity of inhalation air volume	$C_a$	J/K	6.79

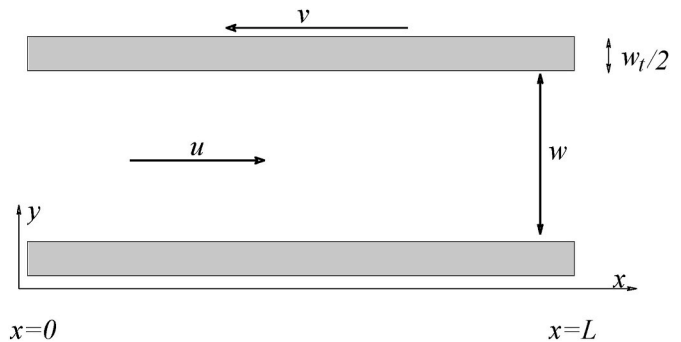


**Fig. 3.** A channel through the MT structure where the air flow is in the  $x$ -direction and enters with ambient conditions on the left-hand side, where  $x = 0$ . The channel has width  $w$  and length  $L$  and air flows at velocity  $u$ ,  $v$  denotes the effective blood velocity in the tissue, which has the local temperature  $T_w$ , while the air has temperature  $T(x, t)$ , where  $t$  is the time. The relevant width of the tissue wall is half the total width  $w_t$ , because there is another channel on the other side that also has thermal exchange with the tissue.

independent channels.

The heat capacity of the MT cannot provide all heat needed to warm and humidify the incoming air. Over time the net energy loss from the MT to the surroundings must then be balanced by heat from lower down the respiratory tract and/or blood flowing through the MT.

As the inhaled air passes through the MT, the air temperature will gradually increase to the deep body temperature (Huntley et al., 1984). In parallel, the MT will cool until it becomes close to the air temperature along the temperature gradient that will result. If the inhaled air is fully conditioned in the MT, there is no net heat or water transport from the rest of the respiratory tract, and all the energy must come from the MT blood supply. However, in reality, some energy must still be supplied by the respiratory tract beyond the MTs as the air temperature will only approach body temperature asymptotically, and for this reason the air that enters the MT during expiration will always be somewhat warmer than the air leaving it during inhalation.

Fig. 3 shows a single channel through the MT structure. We measure the distance from the anterior end of the MT mass (at the left-hand side,  $x = 0$ ) to the posterior end of the MT mass at  $x = L$ . During inhalation the MT is a countercurrent heat exchanger both in the sense that the arterial blood within the wall likely flows counter to the air and in the sense that arterial blood flows counter to the venous blood (Folkow et al., 1988), also inside the wall. The air flow velocity will also vary in the transverse direction  $y$ , but we will use the  $y$ -averaged air velocity,  $u$ . The diffusion time across the channel in this situation is smaller than the transit time along the channel. This means that a diffusing particle (or an amount of heat) will sometimes be on a fast streamline and sometimes on a slow one, but on the average it will move along with the mean air velocity.

In real MT channels the width will vary with  $x$ , while the model assumes a constant width channel. Since the thermal exchange will be dominated by the narrowest part of the MT channels we use the minimal  $w$ -value from the densest tomogram sections. The true lengths of the MT channels are also longer than our effective length  $L$ , measured over the densest part of the MT mass.

### 3.1. Air temperature and humidity

In the following we introduce the model used to describe the air and tissue temperature changes with time. For details of the derivations, see [Appendix C](#).

During inhalation the local temperature  $T(x, y, t)$  will vary both with time and position  $(x, y)$ . It will increase from a minimum value in the channel center to the wall temperature  $T_w$ , because heat is supplied from the walls. In laminar flow, the transverse variation of  $T$  with  $y$  may be approximated by a parabolic function. The hydrodynamics of straight-channel flow with the velocities, lengths and viscosity involved in our case is that of laminar and not turbulent flow ([Batchelor, 1967](#)). So, the transport of heat and vapor across the flow direction will be governed by diffusion alone, and not by transverse advection.

The air temperature is governed by the advection-diffusion equation, which describes the full variation with both  $x$ ,  $y$  and time  $t$ . When averaged in the  $y$ -direction this equation becomes

$$\frac{\partial \bar{T}}{\partial x} = -\frac{\bar{T} - T_w}{l}, \quad (1)$$

which applies to the  $y$ -averaged channel temperature  $\bar{T}$ , see [Appendix C](#). The characteristic length

$$l = \frac{u}{12D_t} w^2 \quad (2)$$

depends on the flow velocity  $u$ , the thermal diffusivity,  $D_t$ , and  $w$ , the width of the turbinate channels. Solving Eq. (1) with respect to  $\bar{T}$  will produce a solution which is given by  $T_w(x, t)$ . The average air temperature is thus given by the wall temperature at each instant in time. During inhalation the boundary condition on the outer end of the turbinates is  $\bar{T}(0, t) = T_a$ .

During exhalation the air velocity changes so that  $u \rightarrow -u$ , and correspondingly  $l \rightarrow -l$  in Eq. (1). Using this simple replacement we are ignoring the small volume difference of the inhaled and expired airflow. Apart from that, the mathematical description of the exhalation remains unchanged compared to that of the inhalation process. During expiration the boundary condition is on the inner end of the turbinates, and is given by  $\bar{T}(L, t) = T_b$ .

The thermal diffusivity  $D_t = 2.5 \cdot 10^{-5} \text{ m}^2/\text{s}$  ([Engineering toolbox Air, 2020](#)). It should be noted that since the mass diffusivity of water vapor in air is  $D_m = 2.4 \cdot 10^{-5} \text{ m}^2/\text{s}$  ([ToolBox, 2020](#)), the humidity variations are also described by Eq. (1), only with  $\bar{T}$  replaced by the vapor density.

The air flow velocity,  $u$ , is the volume flow  $Q$  into the lung divided by the cross sectional area that is available for transport. [Table 1](#) gives the tidal lung volume,  $V_t = 6.3 \text{ l}$  at body temperature and pressure saturated with water (BTPS), see [Appendix A.2](#). This is the volume that leaves the lung by exhalation. This volume is larger than the inhaled volume because it is both heated and moistened. Working backwards, subtracting the volume increase, we obtain the inhaled air volume  $V_i = 5.2 \text{ l}$  (5.8 l) for Eb (Mm) at ambient temperature and pressure, saturated with water (ATP). The time for the seal to draw its breath (inhalation duration)  $t_{br} = 1.1 \text{ s}$ . From this, we compute the volume flow  $Q = V_i/t_{br}$ . The area available for transport is  $A_a$ , the cross-sectional area of air in the structure shown in [Fig. 1](#), cf. [Table 1](#). The air flow velocity becomes particular for each seal, since the value of  $A_a$  is characteristic for each species. We obtain  $u = Q/A_a = 2.3 \text{ m/s}$  (4.1 m/s) for Eb (Mm).

In order to interpret the length  $l$ , consider the hypothetical situation that the entire MT remains at body temperature during air passage. In this case Eq. (1) may be solved to give the difference  $\Delta T_{in} = T_b - T_{in}$  between the inhaled air and the deep body temperature:

$$\Delta T_{in} = (T_b - T_a)e^{-L/l}. \quad (3)$$

If we require that  $\Delta T_{in}$  be close to deep body temperature, say  $\Delta T_{in} < 2^\circ\text{C}$ , the above equation dictates that the turbinate length

$$L > l \ln \left( \frac{T_b - T_a}{\Delta T_{in}} \right) = \begin{cases} 1.04 & \text{cm for Mm } (L = 2 \text{ cm}) \\ 0.27 & \text{cm for Eb } (L = 2.5 \text{ cm}) \end{cases}, \quad (4)$$

where the values in the parenthesis are the measured ones given in [Table 1](#). Since the tissue is not at constant temperature, but will be cooled down by the air, the actual condition will be stricter. As we will see, the modeled values for Eb yield  $\Delta T_{in} < 2^\circ\text{C}$ , but  $\Delta T_{in} > 2^\circ\text{C}$  for Mm, i.e. Eb is able to bring the inhaled gas closer to its deep body temperature, by the time it leaves the MT.

### 3.2. Tissue temperature and blood flow

The nasal mucosa is richly vascularized with a vessel density that far exceeds that required for supply of oxygen ( $\text{O}_2$ ) and nutrients. The vessels thus serve additional purposes. Their close proximity to the respiratory airstream ( $< 100 \mu\text{m}$ ) means that there is rapid thermal exchange between the blood and the air (the heat diffusion time over this length is of the order 0.03 s). The venous blood occupies a cross-sectional area that is a factor  $\sim 25\text{--}30$  larger than that of the arterial blood, and the venous blood flow is therefore relatively slow ([Folkow et al., 1988](#)). The arterial blood will therefore support a significantly larger energy flux. In [Appendix C.3](#) we show that the thermal relaxation time across the channel walls is  $\sim 0.03 \text{ s}$ . This means that on the time scale of the breathing period, transverse temperature gradients inside the walls may be neglected. For these reasons we consider the venous blood along with the tissue as a stationary heat absorber.

In [Appendix C](#) we show that the wall temperature depends on time via the equation

$$\frac{\partial T_w}{\partial t} = \frac{\Delta \bar{T}}{\tau_0} = \frac{\bar{T} - T_w}{\tau_0} + v \frac{\partial T_w}{\partial x}, \quad (5)$$

which describes both the inhalation and exhalation processes in which  $v$  stays the same. Here  $v = f v_b$  where  $v_b$  is the actual blood velocity in the mucosal arterioles and  $f$  the ratio of the arterial blood volume to the bone and tissue volume. If the flux of blood were distributed homogeneously throughout the entire tissue volume, rather than being restricted to flow in the arterioles, it would move with the velocity  $v$ . The fact that it only flows in the arterioles with a velocity  $v_b$  means that  $v_b > v$ .

The arterioles can only support a limited blood flow velocity, which may act as a constraint on the  $v$ -values. In the simulations, however, we place no limitation on  $v$  and find its maximum value to be  $v_{\max} \approx 2.0 \text{ mm/s}$  at the lowest ambient temperatures. When  $f \sim 1\%$  the maximum  $v_b \sim 20 \text{ cm/s}$ , which is quite reasonable given normal arterial/arteriolar blood velocities ([Stanfield and Germann, 2008](#)).

The characteristic time

$$\tau_0 = \frac{c_w w w_t}{12(1 + \alpha)\kappa}. \quad (6)$$

is linked to diffusion across the channel width and  $c_w$  is the heat capacity per unit volume of the wet tissue layer. Using the values taken from ([Popovic and Minceva, 2020](#)) the heat capacity per volume  $c_w = 3.48 \text{ MJ}/(\text{m}^3\text{K})$ . Here  $\kappa$  is the thermal conductivity,  $w_t$  is the tissue width, cf. [Fig. 3](#), and  $\alpha$  is the ratio of the latent heat (evaporation) to the heat that goes into the air. In [Appendix C.2](#) we show that  $\alpha = m_w \Delta H / (C_a (T_b - T_a)) \approx 2.2$  (3.9) for Er (Mm), where  $\Delta H$  is the latent heat of evaporation of water per unit mass and  $C_a$  the heat capacity of the inhaled air. The value of  $\tau_0$  becomes 0.35 s (0.49 s) for Eb (Mm).

The  $v$ -term represents the net heating of the turbinates by blood flowing from the posterior/inner to the anterior/outer part of the turbinates (counter-current flow compared to the inhaled air) at a volume-averaged velocity,  $v$ . This term appears as a positive source term for  $T_w$ . The blood enters the turbinates at  $x = L$ , where the tissue temperature obeys

$$T_w(L, t) = T_b. \quad (7)$$

Adjustment of the blood flow rate is subject to the condition that the anterior turbinate end is kept above some threshold value  $T_{wt} \lesssim 0^\circ\text{C}$ . We assume the critical value to avoid freezing is  $T_{wt} = -2^\circ\text{C}$ . In the simulations  $\nu$  is found by a search algorithm that identifies the minimal  $\nu$  that satisfies this condition, if such a value exists. The reason it may not exist is that the blood flow cannot heat the turbinates above body temperature. When the channel width is too large, the time needed for heat and vapor to diffuse across it will be too large to bring it to body conditions, even when  $T_w = T_b$ . This happens for the Mm even at its normal habitat temperature unless tissue congestion, which gives a smaller channel width, is included in the modeling by a corresponding change in  $w$  and  $w_t$ .

### 3.3. Ice formation

It would be inconsistent to allow for significant sub-zero temperatures in the anterior parts of the MT without allowing ice formation there. In order to include the effect of ice formation in the model it suffices to note that as water freezes on the MT mucosal surface it will give off latent heat so as to maintain the temperature of the underlying tissue above the freezing point. The water could be supplied from the mucosal blood vessels by an osmotic driving force based on a solute concentration in the surface fluid (Widdicombe, 1997), in addition to water supply from capillary filtration, glandular tissue and condensation of water vapor from lung air. As the freezing progresses the solute concentration will increase and depress the freezing point  $T_f$  to  $-2^\circ\text{C}$  of the remaining solution. This process may be described by an effective heat capacity per unit area of the wall

$$C_{w\text{ eff}} = c_w w_t + \Delta H_{ice} \frac{\rho_w h}{T_f} \quad (8)$$

where the latent heat of melting  $\Delta H_{ice} = 0.334 \text{ MJ/kg}$  and  $h$  is the thickness of the liquid film before freezing. Defining

$$\gamma = 1 + \frac{\Delta H_{ice} \rho_w h}{T_f c_w w_t} \quad (9)$$

Eq. (8) may be written  $C_{w\text{ eff}} = \gamma c_w w_t$ , which may be solved for  $h$  to give  $h = 6(\gamma - 1) \mu\text{m}$  if the physical parameters are used. Such a liquid film may well have a viscosity significantly above that of pure water, and with the presence of polymers also acquire a finite yield stress below which it will not flow at all. For these reasons a liquid layer of  $h \sim 100 \mu\text{m}$  may assumed to be stable under the action of the viscous shear forces of the passing air.

Freezing will primarily take place in the anterior part of the MT, where the channels widen to  $w \sim 1 \text{ mm}$  or more (our observations based on CT data), and where such a film thickness may exist. So in the model we shall take  $h = 114 \mu\text{m}$  corresponding to  $\gamma = 20$ . In Eq. (6)  $\tau \propto c_w$ , and the freezing effect is included by the replacement  $c_w \rightarrow \gamma c_w$  at places where  $T_w < 0$ . The resulting temperature profiles will not be sensitive to small variations around this  $\gamma$ -value as long as liquid water remains available in the MT channel. Note that the temperature dependence in the heat capacity does not violate energy conservation as it will have the same value when the temperature is rising as when it is dropping.

## 4. Results

All temperature profiles through the MT are obtained by integrating Eq. (1) and Eq. (5) numerically starting with the initial condition

$$T_w(x, 0) = T_b. \quad (10)$$

In order to describe the change from inhalation to exhalation the sign of  $u$  was changed in Eq. (2); a full breathing cycle was thus computed by

integrating Eq.(1) for a period  $t_{br}$  and then for the same period of time with the opposite  $u$ -value. The time-step  $dt$  was set to  $t_{br}/(4\nu)$  in order for the code to be stable. Unless otherwise stated we integrated over 10 breathing cycles to reach a steady state where the sensitivity to this particular initial condition is lost.

Fig. 4 shows how the blood-flow adjusts to the ambient temperature given the no-freezing condition. In the cases where  $\nu = 0$  all the energy supply comes from the post-turbinate respiratory tract. This must be the case because the inhaled air (the air by the time it has reached the innermost MTs) is up to  $2^\circ\text{C}$  below the air returning from the lungs, implying an energy input from somewhere beyond the MTs. At  $T_a \geq -15^\circ\text{C}$  the Eb model may satisfy the no-freezing condition with no blood flow at all, although there is the freedom to increase the blood supply, thus increasing the MT temperature above the minimum requirement. As we shall see, this is an option that may be employed to allow for increased energy loss from a thermally stressed animal.

Fig. 4 also shows the hypothetical case where no ice is forming and the blood flow is allowed to reach values  $\sim 0.5 \text{ cm/s}$ . With  $f = 1\%$  this would correspond to real blood flow velocities  $\sim 0.5 \text{ m/s}$ , which is considered unrealistic in small scale arterioles.

At sub-zero temperatures the ice plays an increasing role, reducing the necessary blood supply by more than a factor of 2 at  $T_a < -15^\circ\text{C}$  and making it potentially redundant at  $-15^\circ\text{C} < T_a < 0^\circ\text{C}$ . Note also that for Eb  $\nu$  decreases as  $T_a$  changes from  $-25^\circ\text{C}$  to  $-30^\circ\text{C}$ . This effect is perhaps surprising, but may be understood from the increase in ice formation: as the ambient temperature is lowered, the amount of the ice and the energy it absorbs in freezing, increases, and less blood is needed to maintain tissue temperature at the end of the inhalation period.

Fig. 5 shows the temperatures both in the tissue and the air for both species at the end of the expiration and inhalation cycles when  $T_a$  is set to the average habitat values for both species. Note that the no-freezing condition is met at this extreme temperature as well, and freezing will occur only over a few millimeters of the anterior MT. There is a slope discontinuity in the tissue temperature around  $x = 0.2 \text{ cm}$ , which shows where the ice layer stops. In these figures Eb meets the no-freezing condition and conditions the air to body conditions for  $\nu < \nu_{\text{max}}$ , while Mm does not. The Mm inhaled air temperature falls about  $7^\circ\text{C}$  below  $T_b$  at its average habitat temperature, even though the ambient air is much warmer for Mm than for Eb.

The tissue width  $w_t$  includes both the bone and the vascular mucosa that lines the air channels. In life, the nasal mucosa of mammals can increase in thickness through vascular congestion (Widdicombe, 1997). It is possible to adapt the model for Mm so that the air becomes conditioned to within  $2^\circ\text{C}$  of body temperature by increasing  $w_t$  by 70%.

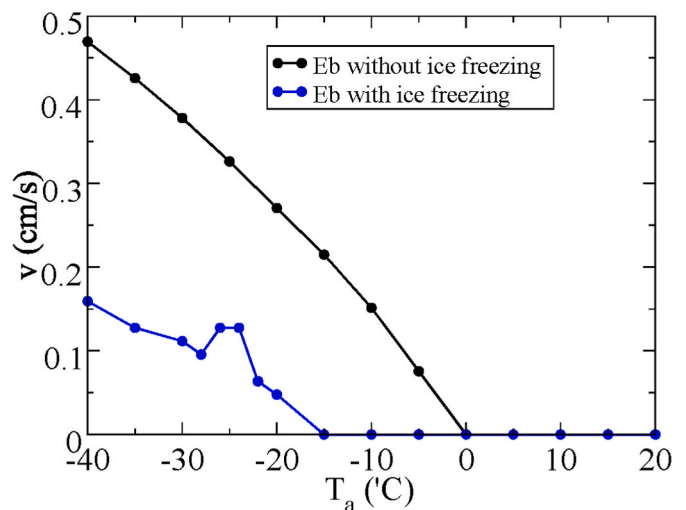
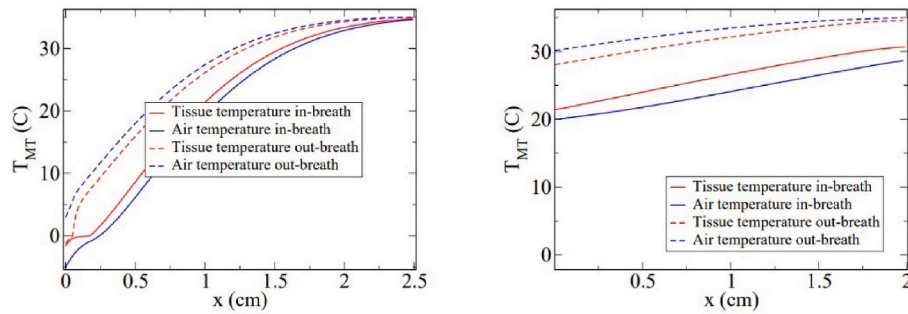


Fig. 4. The effective MT blood velocity  $\nu$  as a function of the ambient air temperature  $T_a$  for Eb.



**Fig. 5.** Modeled temperature profiles for the seals in their natural habitat temperatures. The profiles reflect the situation at the end of the inhalation and expiration. The  $x$ -coordinate measures the distance along the MT wall. Left figure: Eb at  $T_a = -5^\circ\text{C}$ . Right figure: Mm at  $T_a = 20^\circ\text{C}$ . For Mm  $v = v_{\max} = 2$  mm/s, while for Eb  $v = 0$  mm/s. For both seals, deep body temperature is  $35^\circ\text{C}$ . The results shown are those obtained after 10 respiratory cycles.

Within the model, this narrows the air channel widths, increases the heat capacity of the tissues and increases air velocity.

The energy cost of ventilation includes that of the hydrodynamic drag in the airflow through the MT. In Appendix A.3 it is shown that the  $w$ -values given in Table 1 give the power values  $dW/dt = 0.28$  W (0.12 W) for Eb (Mm). These power values increase as  $1/w^3$  as the channel width is decreased, so power consumption will eventually place a lower limit on  $w$ . Even when the Mm tissue width is increased by the factor 1.7 the power  $dW/dt = 1.2$  W, which is still a very small fraction (0.7%) of the BMR (Kleiber, 1961). Fig. 6 shows the temperature profiles for both species in a colder than average environment. For Eb the arctic conditions have become very severe, with  $T_a = -40^\circ\text{C}$ , while for Mm the hypothetical environment is the standard arctic conditions previously modeled for Eb. For Mm the inhaled air temperature falls  $17^\circ\text{C}$  below the deep body temperature, while Eb is able to condition the air to deep body temperature and humidity.

#### 4.1. Effect of eliminating the energy supplied to the MT via the blood flow

Control of the blood flow to the MT region is presumably exercised by vasomotor adjustments to smooth muscle cells in the walls of the supplying sphenopalatine artery, as well as in the two key outlet vessels, the sphenopalatine vein and the dorsal nasal vein. The walls of these vessels are unusually thick compared to those of other veins (Folkow et al., 1988).

Fig. 7 shows  $T_{\text{ex}}(x) = T(x, t_{br})$  if the blood flow velocity is assumed to be  $0.02$  mm/s. This minute supply of arterial blood is insufficient to meet the no-freezing condition, and also to bring the inhaled air to body conditions. Fig. 7 shows the development of the expired air temperature profiles with each breath under this condition when at  $T_a = -40^\circ\text{C}$ . The rightmost Fig. 7 shows the temperature profiles at the end of the 10 cycles.

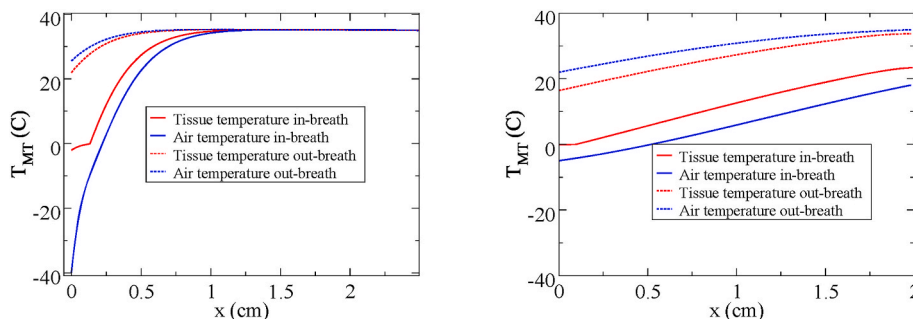


**Fig. 6.** Left figure: the temperature profile along the MT channels of Eb in an extreme arctic environment of  $T_a = -40^\circ\text{C}$ . Right figure: Mm in an arctic  $T_a = -5^\circ\text{C}$  environment. For Mm  $v = v_{\max} = 2$  mm/s, while  $v = 1.6$  mm/s for Eb. In both cases, the results shown are those obtained after 10 respiratory cycles.

#### 4.2. Effect of changing inhalation/exhalation time

Fig. 8 shows the variation of  $T_{\text{ex}} = T(0, t_{br})$  with breath duration when  $v$  is set by the no-freezing condition. In these calculations the tidal volume is fixed, and the air velocity changes according to the changes in  $t_{br}$ . At  $T_a = -40^\circ\text{C}$  the exhaled air temperature decreases with  $t_{br}$ , as the faster breathing causes ice to form over a longer section of the MT. At the same time there is a need for a greater blood flow so as to stop the MT tissue below from freezing. At  $t_{br} = 0.7$  s the blood flow is  $v = 1.9$  mm/s, which is right below the limit which is considered the maximum. This means that only a limited reduction in  $T_{\text{ex}}$  may be obtained by more rapid ventilation since this would eventually lead to freezing of the outer MT. At  $T_a = -20^\circ\text{C}$  a minimum occurs at  $t_{br} = 0.8$  s, while at  $T_a = -5^\circ\text{C}$   $T_{\text{ex}}$  decreases slowly with increasing  $t_{br}$ .

#### 4.3. Energy saving

The energy lost per respiration cycle is

$$\Delta E = A_a \int_0^{t_b} dt [J_{\text{ex}}(t) - J_{\text{in}}(t)] \quad (11)$$

where the duration of the full cycle is  $2t_b$ , and  $J_{\text{ex}}(t)$  and  $J_{\text{in}}(t)$  are the energy fluxes as measured in the channel at the inlet to the MT, i.e. at  $x = 0$ , and where  $A_a$  is the cross-sectional area of the air as defined above. We assume that the duration of the expiration is the same as the inhalation.

The energy density that is advected with the flow has two contributions, one that is given by the heat capacity and the temperature, and one that is given by the latent heat of evaporation/condensation. The latter depends on the vapor pressure, which we shall take to be given by the temperature too, assuming that the air is fully saturated with vapor. The net energy loss in one breathing cycle is

$$J_{\text{ex}}(t) - J_{\text{in}}(t) = [\Delta\rho_w(t)\Delta H + c_a(T_{\text{ex}}(t) - T_a)]u, \quad (12)$$

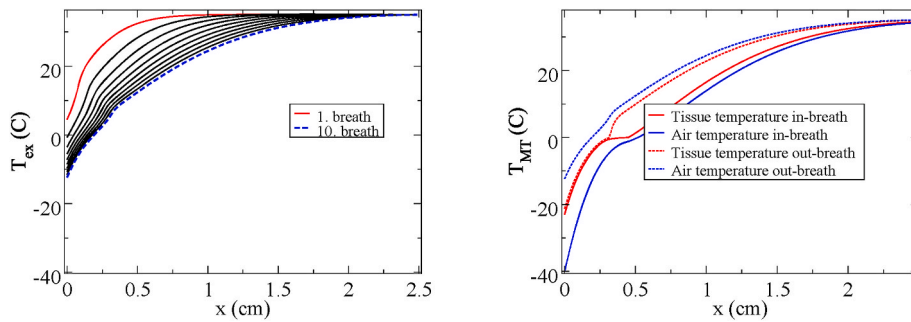


Fig. 7. Modeled effects of reducing the blood supply in Eb to  $v = 0.02$  mm/s. Left figure: The changes of the exhaled air temperature profile over 10 breathing cycles at  $T_a = -40^\circ\text{C}$ . Right figure: Final temperature profiles when  $T_a = -40^\circ\text{C}$ .

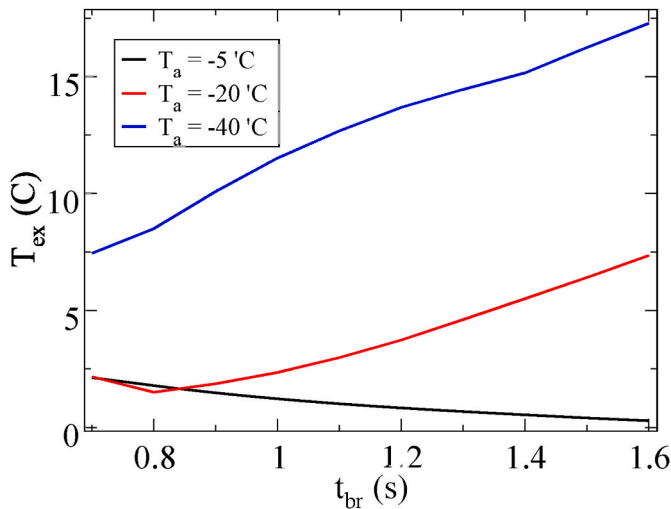


Fig. 8. Modeled exhaled temperature averaged over the expiration period as a function of inhalation time  $t_{br}$  in Eb. Normal inhalation time within the model is taken to be 1.1 s.

where  $T_{ex}(t) = T(0, t)$  during exhalation. Here  $\Delta\rho_w = \rho_w(T_{ex}) - \rho_w(T_a)$  is the mass of water per unit volume leaving the MT at the expiration temperature,  $T_{ex}$ , minus the corresponding incoming quantity, and  $c_a$  is the air heat capacity per unit volume at constant pressure.

Without the MT, the water and air would leave the nose at body temperature and the energy loss takes its maximum value

$$\Delta E(T_b) = A_a u t_{br} [(\rho_w(T_b) - \rho_w(T_a))\Delta H + c_a(T_b - T_a)]. \quad (13)$$

In the presence of the MT, the temperature  $T_{ex}(t)$  and humidity at  $x = 0$  will vary with time, and the above expression must be replaced by

$$\Delta E(T_{ex}) = A_a u \int_0^{t_{br}} dt [(\rho_w(T_{ex}) - \rho_w(T_a))\Delta H + c_a(T_{ex} - T_a)]. \quad (14)$$

Assuming that the air is saturated so that  $\rho_w(T_{ex})$  is just a function of temperature, the vapor mass density may be calculated by the standard Clausius-Clapeyron equation

$$\rho_w(T) = \rho_b \frac{T_b}{T} e^{-m\Delta H \left( \frac{1}{kT} - \frac{1}{kT_b} \right)} \quad (15)$$

where  $k$  is Boltzmann's constant,  $m$  the mass of a water molecule,  $\rho_b$  the equilibrium vapor density at  $T_b$  and the  $T$ 's are absolute temperatures (units of K). The corresponding expression for the amount  $\Delta M_w$  of water saved is

$$\Delta M_w(T_{ex}) = A_a u \int_0^{t_{br}} dt [(\rho_w(T_{ex}) - \rho_w(T_a))]. \quad (16)$$

The energy saving due to the MT structure can be expressed as

$$\text{Energy saved} = \frac{\Delta E(T_b) - \Delta E(T_{ex})}{\Delta E(T_b)} \quad (17)$$

where  $\Delta E(T_b)$  and  $\Delta E(T_{ex})$ , which are given by Eq. (13) and Eq. (14), are integrated numerically over time. A corresponding expression for the water savings based on Eq. (16) would allow a calculation of the water loss. However, as  $\Delta H$  and  $c_a$  are constants, the water and energy losses in our model will behave similarly and both decay monotonously with decreasing  $T_{ex}$ . For this reason we limit the calculations to the energy loss.

#### 4.4. Energy recovery and expired air temperatures

The energy which is conserved due to the MT heat exchange process is plotted against  $T_a$  in Fig. 9 for both Eb (blue) and Mm (red). In addition, the effect of reducing the tidal volume by a factor 1/3 and ignoring the ice formation is shown. Note that the energy saving of Mm, plotted only for the above-zero temperatures, is significantly lower than that of Eb. As in Figs. 5 and 6 we have set  $v = v_{max}$  for Mm in order to bring the inhaled air as close as possible to body conditions. Fig. 9 also

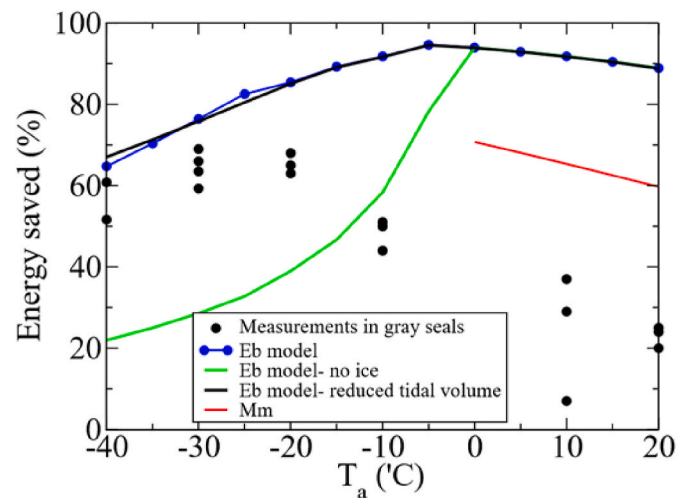


Fig. 9. The relative energy saving given in Eq. (17) as a function of the ambient air temperature  $T_a$  for Eb and Mm. The blue and black curves show the modeled Eb values, while the green curve shows the hypothetical case where no ice forms and the blood velocity is unconstrained ( $v > v_{max}$ ). For the Mm curve  $v = v_{max}$ . Corresponding calculations based on measurements (●) in 3 grey seals (Folkow and Blix, 1987).

shows calculations based on measurements in grey seals (Folkow and Blix, 1987) which may display similar body mass and tidal volume as both Eb and Mm. The grey seal occurs in northerly waters but is not considered an arctic species. Its MT development is intermediate between that of Eb and Mm (Mason et al., 2020).

In Fig. 10 the exhaled air temperature averaged over an out-breath period (after the steady state is reached) is shown as a function of  $T_a$ . The averaged  $T_{ex}$  is closely related to the energy saving. In fact, if the vapor density in Eq. (15) is linearized in  $T$ , the energy saving and averaged exhaled air temperature become linearly related, and the recovered energy increases as the averaged expired air temperature decreases.

In Fig. 10, measurements made on grey seals (Folkow and Blix, 1987) are seen to coincide with the modeled values at low  $T_a$ . Fig. 10 also shows the effect on  $T_{ex}$  of reducing the tidal volume while keeping  $t_{br}$  fixed (i.e., as seals do under resting conditions (Folkow and Blix, 1987)). The effect of this is observed to be negligible. Without the ice formation, however, the exhaled air temperatures are  $\sim 15^\circ\text{C}$  above the range of the measured values for the grey seal at low  $T_a$ .

## 5. Discussion and conclusion

The modeling strongly suggests that the respiratory turbinates have evolved to enable the seals both to bring the inhaled air temperature and humidity close to deep body conditions, and to maintain body heat, under prevailing environmental conditions. The model is based on the notion that the blood flow through the turbinate is controlled in order keep the turbinate from freezing. This condition gives a minimum blood velocity, which sets a rate for the minimal rate at which heat and water is lost.

Among the many simplifications we have made, our model only considers the main mass of densely-packed maxilloturbinates, which does not include the less compact regions in the anterior and posterior directions. We have ignored any effect of the anterior nasal cavity, between maxilloturbinates and nostrils, in warming the inhaled air (Huntley et al., 1984), and we have also ignored the effects of any changes in flow pattern of venous blood, which might be possible given that there is more than one venous outlet from the nasal region (Folkow et al., 1988).

At low ambient temperatures the model prediction for the expired air temperatures in the arctic bearded seal agree well with measured values in grey seals, provided the effect of ice formation on the surface of the

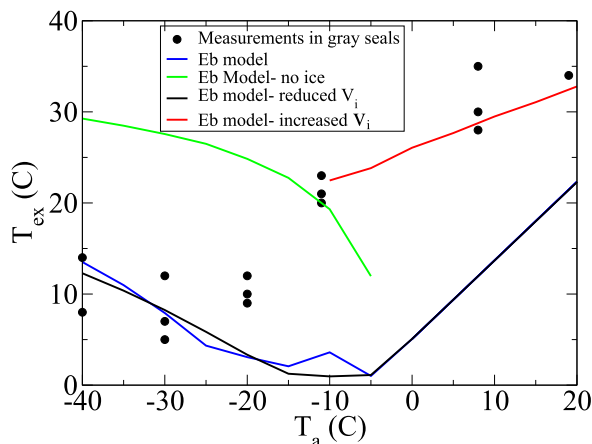


Fig. 10. Modeled exhaled temperatures for Eb, averaged over the exhalation period, as a function of the ambient temperature  $T_a$  (blue line). The black curve shows the effect of reducing the tidal volume,  $V_i \rightarrow V_i/3$ , the red curve the effect of increasing the blood flow to  $v = 1.0\text{--}1.15$  mm/s. The green line shows the hypothetical effect of omitting the ice formation on the distal MTs. Corresponding measurements ( $\bullet$ ) taken from 3 grey seals (Folkow and Blix, 1987).

anterior turbinates is included. At low ambient temperatures the ice plays a crucial role as a heat reservoir, reducing the blood flow required to maintain the tissue beneath the ice above freezing. The reason for this is the latent heat given off during the freezing that takes place during inhalation.

At low/intermediate temperatures ( $T_a \geq -20^\circ\text{C}$ ) the model assuming minimized blood flow produces lower exhaled air temperatures than has been measured in grey seals, and energy conservation at low temperatures is higher, as is seen in Fig. 9. This would be expected based on the more complex MT structure of *Erignathus* compared to the grey seals (Mason et al., 2020). However, the model values agree with the measurements if we assume that blood flow is increased, as is physiologically possible, and a likely mechanism for the control of heat loss in the animal (Folkow et al., 1988). In other words, this is a mechanism for dissipating excess heat, at the expense of water loss.

Fig. 6 shows that *Erignathus* may cope with conditions of  $T_a = -40^\circ\text{C}$  without losing the ability to condition the air for the lungs, provided that ice may form in the anterior turbinate region. *Monachus*, on the other hand, is only able to equilibrate the air to body conditions above  $T_a = -5^\circ\text{C}$  if we assume that nasal mucosa is engorged with blood. This is due to the larger channel widths and larger air flow velocity predicted on the basis of the anatomy of *Monachus*. Fig. 9 shows that the energy saving of *Erignathus* is superior to that of *Monachus* in the range of ambient temperatures from arctic to tropical.

### 5.1. Optimization through changing blood flow

Fig. 10 shows that around the typical habitat temperature of  $-5^\circ\text{C}$  the range of possible values for exhaled air temperatures (the distance between the red and the blue curves) that is controlled by the blood velocity, is at its largest. At very low ambient temperatures the animal has little choice but to increase the blood flow to avoid freezing, and at high temperature the range of exhaled temperatures narrows again, since it can never be lower than the ambient temperature. Correspondingly, the potential variability in energy loss is largest around  $-5^\circ\text{C}$ . This indicates that the turbinates have evolved to a greater adaptability right at the typical *Erignathus* habitat temperature. The adaptability in the energy release may be understood from the fact that the need to conserve energy will vary with the level of activity and the metabolism of the animal.

The red curve in Fig. 10 shows the result of fitting the model to the measured  $T_{ex}$  values in the ambient temperature range  $-10^\circ\text{C} \leq T_a \leq 20^\circ\text{C}$ . The fact that the required blood velocities are inside the range  $0 < v < 2$  mm/s, allowed in the model, serves to validate it. On the other hand, the fact that the resulting  $v$  values are almost constant over a  $T_a$ -range of  $30^\circ\text{C}$  is interesting and suggests that the  $v \approx 1$  mm/s value may be physiologically optimal also relative to other functions. It should be noted that we have not attempted to model different options for the MT blood flow pattern, based on possible use of two alternative venous drainages (Folkow et al., 1988), which may also affect heat exchange processes.

Increasing the blood flow rate through the turbinate structure is distinct from vascular congestion, which refers to increasing the total amount of blood within the turbinate mucosa at any given instant in time. In principle, animals could alter either or both of these parameters through appropriate dilatation or constriction of the vessels supplying and draining the tissue. Neural control of these blood vessels could therefore be exerted to optimize the nasal passageways for:

1. Maximal heat and water loss if the animal is hyperthermic (maximal blood flow-rate, minimal congestion),
2. Maximal heat and water conservation (minimal blood flow-rate),
3. Or for fully conditioning the inhaled air to body conditions at the posterior end of the turbinates (maximal blood flow rate, maximal congestion).

In case 2 of maximal conservation, the minimal blood flow-rate depends on the congestion. For *Erignathus* no congestion at all, or a tissue congestion by 10%, already optimizes the conservation, while congestion improves conservation in *Monachus*. High levels of congestion come at the cost of increased work of breathing, although this might only become significant when the air channels are very narrow (see Appendix A.3).

While the control of blood flow has a large potential to affect the heat and water loss, variations in the breath duration and tidal volume have less effect. In this context, it is relevant to note that pinnipeds in general seem to not pant in response to hyperthermia (Matsuura and Whittow, 1974). At extreme ambient temperatures ( $-40^{\circ}\text{C}$ ), however, the model suggests that *Erignathus* could improve conservation to some extent by decreasing the breath duration at the cost of elevated blood flow rates.

Folkow and Blix (1989) studied the effect of changing the water temperature instead of the ambient air temperature, and found that harp seals (*Pagophilus groenlandicus*) immersed in cold water ( $2^{\circ}\text{C}$ ) have a  $T_{ex}$  that is  $10^{\circ}\text{C}$  lower than when immersed in warm water ( $25^{\circ}\text{C}$ ). The seals inhaled air of the same temperature ( $T_a = 0^{\circ}\text{C}$ ) in both situations (Fig. 10 in (Folkow and Blix, 1989)). This observation supports the physiological adaptability predicted by our model.

## 5.2. Water versus heat conservation

Based on latitudinal differences in MT-complexity between seal species, Mason and coworkers argued (Mason et al., 2020) that the heat conservation is likely more important than the water conservation, as also indicated by the observations described above (Folkow and Blix, 1989) and the lack of adjustments in  $T_{ex}$  when the hydration state of seals was experimentally manipulated (Skog and Folkow, 1994). Thus, Fig. 10 shows that at  $T_a > 5^{\circ}\text{C}$ , the measured exhaled air temperature in grey seals is  $10\text{--}15^{\circ}\text{C}$  higher than the predicted minimum temperature of our model (based on the *Erignathus* MT anatomy). The warmer the exhaled air temperature, the more water is lost. Assuming that the grey seal is capable of similar heat conservation to *Erignathus*, this indicates that the seal prioritizes the dissipation of excess heat over the associated cost of also losing water, which is in agreement with these conclusions. However, the MT may respond both to the need of water and heat conservation. Depending both on internal conditions, such as fasting, and on environmental conditions, the animal may need to prioritize either heat or water conservation; in either case the MT may serve the purpose.

Our model is based on the assumption that heat and water loss go hand-in-hand in the sense that heat loss implies water loss and vice versa. In the channels through the turbinates the transport of heat and humidity is governed by diffusivities that are almost equal, so that the water and heat densities are described by the same equations.

For *Monachus*, the absolute humidity of the inhaled air in its normal environment is about twice as high as in an arctic one. For this reason, there is a much smaller potential for water loss by breathing. Yet, the MT

## Appendix A. Physiological and anatomical data

In the following we describe how the physiological measurements were made and derive the amount of evaporated water  $m_w$ , as well as the energy spent by overcoming the hydrodynamic drag involved in breathing.

### Appendix A.1. Physiological data

Physiological data are not abundant for these seals, and are therefore partly taken from the harp seal (*Pagophilus groenlandicus*) (Folkow et al., 1988; Folkow and Blix, 1989), the northern elephant seal (*Mirounga angustirostris*), see Huntley et al. (1984), and the grey seal (*Halichoerus grypus*) (Folkow et al., 1988; Reed et al., 1994; Folkow and Blix, 1987). We have assumed that animals have the same mean body mass, 180 kg, and the same total lung capacity of 14.6 l (Kooyman, 1989). Rather than the total lung volume, we consider the tidal volume as most relevant for the analysis of respiration. The tidal volume listed in Table 1 represents the volume of air that is shifted through the nasal cavity during each exhalation. We have chosen to use values measured on seals resting in water (Reed et al., 1994).

organ of the subtropical *Monachus* may still play some role in the conservation of water and heat.

### 5.3. The effect of apnea

Seals are known to economize their energy consumption during diving by reducing their metabolic rate. Apnea of up to 20 min may occur during sleeping as well (Castellini, 1996). During these periods, the heart rate slows and peripheral vascular resistance rises. When the maxilloturbinates are initially at body temperature, which they might be following a long dive with nostrils closed, heat and water conservation is best only after some  $\sim 10$  breathing cycles (see Fig. 7). However, measurements of  $T_{ex}$  in harp seals after dives (Folkow and Blix, 1989) have shown that the exhaled air temperatures are almost the same before and after the dives. This indicates that the seal shuts off the supply of warm blood to the turbinates during diving, thus conserving heat and water after the dive without the losses linked to the process of recooling the turbinates. This strategy will be most efficient at very low  $T_a$ . The effects of shorter apnea  $\sim 1$  min in fasting elephant seals have been found to reduce water loss by up to 40% (Lester and Costa, 2006) in conjunction with a corresponding reduction in metabolic rate. This is consistent with the above findings.

## CRediT authorship statement

Eirik G. Flekkøy: modeling, theory and writing draft, Lars P. Folkow: data production and conceptualization, Signe Kjelstrup: theory development, Matthew J Mason: data production, theory development and conceptualization, and Øivind Wilhelmsen: conceptualization.

## Funding sources

The funding is provided by The Research Council of Norway, through its Center of Excellence Funding Scheme, PoreLab, project number 262644.

## Declaration of competing interest

There are no competing interests pertaining to this publication.

## Acknowledgement

EGF, SK and ØW are thanking the Research Council of Norway through its Center of Excellence Funding Scheme, PoreLab, project number 262644. We thank Arnoldus Schytte Blix, Øyvind Hammer and Léa Wenger for the use of the CT scan data which they helped to produce. LPF is grateful to the Tromsø Research Foundation for funding of the project *Energy efficiency of mechanisms for respiratory heat and water exchange in arctic mammals*.

Anatomical values based on the MT structures of seals were taken from CT scans made by [Mason et al. \(2020\)](#). All measurements of *Erignathus barbatus* were made from scans of the single specimen available. Measurements of *Monachus monachus* were mean values from two specimens.

Channel width values were calculated from CT cross-sections which had been reoriented so as to pass through the densest part of the maxilloturbinate mass. Details of how these cross-sections were obtained are given in [Mason et al. \(2020\)](#). A perimeter was closely drawn around the whole maxilloturbinate mass in these cross-sections, including both air and tissue and including both left and right sides of the nose, and the area contained within this was measured and designated as  $A$ . The area within  $A$  that is occupied by tissue (i.e. the black pixels in [Fig. 1](#)), representing the maxilloturbinate bone plus any residual soft tissue covering it, was calculated and designated  $A_b$ . The perimeter of the turbinates within the cross-section,  $P$ , had previously been calculated by [Mason et al. \(2020\)](#). We then assumed that the complex structure of the maxilloturbinates could be approximated as a very thin sheet, bent and convoluted so as to enclose a very thin sheet of air.

Using the geometric relation that the cross-sectional area of the air (tissue)  $A_a = Pw/2$  ( $A_b = Pw_t/2$ ) where  $P$  is the common perimeter, we can use the area and perimeter measurements to obtain the bone width and the width of the channels as  $w = 2A_a/P$  and  $w_t = 2A_b/P$ .

The effective path length was measured directly from the 3D scans by locating the ends of the channel in the cross-sections that were taken in the direction along the flow: see [Mason et al. \(2020\)](#).

The anterior and posterior regions of the maxilloturbinates contain a small number of large, structural elements and are hence much more ‘open’ than the central region, where the maxilloturbinates are densely packed and where most heat and water exchange presumably occurs. The effective turbinate lengths,  $L$ , used in the model were taken to be the lengths of the air channels passing through the dense, central part of the maxilloturbinate mass. These values were estimates based on multiple measurements made directly on scaled tomogram sections in horizontal and sagittal planes, using Stradview 6.13.

#### Appendix A.2. Evaporated water mass $m_w$

During inhalation, we assume that the outside air is saturated with water as it passes through the MTs and reaches the pharynx at 35°C. Here we calculate the added water mass  $m_w$  and the outside initial volume  $V_i$  of air that ends up at a volume  $V_2 = 6.3$  l after inhalation. The saturated water vapor pressure as a function of temperature  $P_w(T)$  is taken from [Poling et al. \(2001\)](#). The values we need are  $P_w(T_b) = 5879$  Pa,  $P_w(20^\circ\text{C}) = 2340$  Pa and  $P_w(-5^\circ\text{C}) = 426$  Pa.

Using the ideal gas law  $PV = NkT$  and the fact that the number of air molecules (excluding the water molecules) is conserved during inhalation, we can write

$$\frac{(P_0 - P_w(T_a))V_i}{T_a} = \frac{(P_0 - P_w(T_b))V_2}{T_b} \quad (\text{A.1})$$

where  $P_0 = 100$  kPa is the atmospheric pressure. This equation gives the initial volume

$$V_i = \frac{(P_0 - P_w(T_b))T_a V_2}{(P_0 - P_w(T_a))T_b} \approx 5.2 \text{ l Eb (5.8 l for Mm)}, \quad (\text{A.2})$$

Again, using the ideal gas law, we may calculate the added number of water molecules

$$\Delta N_w = \frac{P_w(T_b)V_2}{kT_b} - \frac{P_w(T_a)V_i}{kT_a}, \quad (\text{A.3})$$

as well as the corresponding added water mass

$$m_w = m\Delta N_w = \frac{m}{k} \frac{V_2}{T_b} \left( P_w(T_b) - \frac{P_0 - P_w(T_b)}{P_0 - P_w(T_a)} P_w(T_a) \right), \quad (\text{A.4})$$

where  $m$  is the mass of a water molecule. Now, since  $m/k \approx 2.44$  gK/J, we get  $m_w = 0.24$  g (0.16 g) for Eb (Mm).

#### Appendix A.3. Viscous dissipation

The work performed by the respiratory muscles to overcome the pressure drop along the airflow through the MT structures gives an idea of metabolic cost of breathing. The pressure drop depends on the air viscosity  $\mu_a$ , the channel width  $w$  and length  $L$  as well as the volume flux  $Q$  during in- and exhalation. Since the flow velocities are moderate, the Reynolds number is well below the critical threshold where turbulence sets in, so it is safe to assume laminar flow. In this case, the pressure drop is given by Darcy’s law ([Batchelor, 1967](#))

$$\Delta P = \frac{12\mu L}{w^2} u \quad (\text{A.5})$$

and the corresponding power, or work per unit time,  $dW/dt$  is

$$\frac{dW}{dt} = Q\Delta P = \frac{12\mu LA_a}{w^2} u^2 \quad (\text{A.6})$$

where cross-sectional area  $A_a$  of the air enters because it determines the mean flow velocity  $u$  through the channels. If  $Q$  is fixed and  $w$  is changed,  $dW/dt \propto 1/w^3$  since  $u \propto Q/w$  and  $A \propto w$ . Using the range of  $w$ -values and air viscosity  $\mu = 1.9 \cdot 10^{-5}$  Pa s we find the power values  $dW/dt = 0.66$  W for Eb, and  $dW/dt = 0.28$  W for Mm. These values represent 0.40% and 0.17%, respectively, of the predicted basal metabolic rate for a 180 kg mammal ([Kleiber,](#)

1961).

## Appendix B. Ambient conditions

The inhaled air temperature was set equal to the ambient temperature ( $T_a$ ) for the selected species. These temperatures were estimated from distribution maps for Mm seals (Kenyon, 1981) and Eb seals (Burns, 1981), combined with an annual global temperature map (Matsuura, 2020). Based on data for northern elephant seals (Huntley et al., 1984), the air temperature is 5–10 °C higher than  $T_a$  just inside the nostril and close to deep body temperature,  $T_b = 35$  °C at the pharynx.

According to these considerations, the mean ambient air temperature in the subtropical zone was estimated to 20 °C (Kenyon, 1981), while the corresponding temperature of the arctic region was -5°C (Burns, 1981; Matsuura, 2020). The temperature at the level of the pharynx was assumed to be  $T_b = 35$ °C in both seals.

## Appendix C. Temperature profiles along the turbinate channels

During inhalation the air is gradually heated and moistened along the MT channels. Starting at the ambient temperature the air is heated gradually along its path while at the same time cooling the turbinates. At the posterior end of the MT the air and tissue temperatures will be closer to each other. We have estimated thermal penetration depth of the MT tissue as  $l_s = \sqrt{2D_w t_{br}} \approx 0.6$  mm, if the thermal diffusivity of liquid water is used for  $D_w$ . This depth is larger than  $w_T$ . This means that the tissue temperature may be assumed constant across a turbinate wall in the direction perpendicular to the flow. So, we can take the wall temperature to be a function only of time and the position  $x$  along the flow direction, while the air temperature  $T$  will vary with both  $x$  and the distance  $y$  from the wall, as well as time.

In reality the width of the channels through the turbinates vary with  $x$ , a fact that implies a slower thermal exchange and weaker cooling of its outmost part. For simplicity, we will only consider the constant width case, an approximation that will produce an overestimate of the cooling of the anterior end of the turbinates.

### Appendix C.1. Air temperature

In a channel, such as illustrated in Fig. 3, the air temperature is described by the advection diffusion equation

$$\frac{\partial T}{\partial t} + u \frac{\partial T}{\partial x} = D_i \nabla^2 T \quad (\text{C.1})$$

where  $t$  is the time and  $u$  the mean flow velocity along the channel. During inhalation  $T(x, y, t)$  will increase from a minimum in the center to the wall temperature  $T_w$  because of diffusion. For simplicity we have assumed this transverse variation with  $y$  to be parabolic so that

$$\Delta T = T - T_w = \overline{\Delta T} \frac{6y(w-y)}{w^2} \quad (\text{C.2})$$

where  $\overline{\Delta T}$  is the temperature difference averaged in the  $y$ -direction. Now, the variation is much faster in the  $y$ -direction than in the  $x$  direction since  $L \gg w$ , so we may approximate  $\nabla^2 T \approx \partial^2 T / \partial y^2 = -12\overline{\Delta T} / w^2$ . Using this and averaging the whole equation (C.1) in the  $y$ -direction gives

$$\frac{\partial \overline{T}(x, t)}{\partial t} + u \frac{\partial \overline{T}(x, t)}{\partial x} = -\frac{12}{w^2} \overline{\Delta T}(x, t). \quad (\text{C.3})$$

Introducing the length

$$l = \frac{u}{12D_i} w^2 \quad (\text{C.4})$$

equation (C.3) may then be written

$$\frac{1}{u} \frac{\partial \overline{T}}{\partial t} + \frac{\partial \overline{T}}{\partial x} = -\frac{\overline{\Delta T}}{l}. \quad (\text{C.5})$$

Here we can estimate the order of magnitude of the two leftmost terms

$$\frac{1}{u} \frac{\partial \overline{\Delta T}}{\partial t} \sim \frac{\overline{\Delta T}}{ut_{br}} \ll \frac{\overline{\Delta T}}{L} \sim \frac{\partial \overline{\Delta T}}{\partial x} \quad (\text{C.6})$$

since  $ut_{br} \approx 5$  m while  $L \approx 5$  cm. So, we drop the first term in equation (C.5), which leaves us with

$$\frac{\partial \overline{T}}{\partial x} = -\frac{\overline{T} - T_w}{l}, \quad (\text{C.7})$$

which is Eq. (1). During expiration the flow direction is reversed and  $u \rightarrow -u$  will cause  $l \rightarrow -l$ , which means that the air temperature is now given by

$$\frac{\partial \overline{T}}{\partial x} = \frac{\overline{T} - T_w}{l}. \quad (\text{C.8})$$

The boundary condition is now.  $\bar{T}(L, t) = T_b$

### Appendix C.2. Wall temperature

On the boundary where  $y = w$  the heat from the air per unit area  $q$  is given by Fourier's law

$$q = -\kappa \frac{\partial T}{\partial y} = \frac{6\kappa}{w} \Delta \bar{T}, \quad (C.9)$$

where  $\kappa = 0.024 \text{ J}/(\text{m}^2\text{K})$  is the thermal conductivity of air. The thermal energy of the tissue, on the other hand, goes into warming the air and evaporating water. Neglecting the energy supplied from the blood flow for now, this exchange is described by the following energy balance equation:

$$C_t \frac{\partial T_w}{\partial t} = \frac{6\kappa}{w} \Delta \bar{T} + \Delta H \frac{\partial \rho_w}{\partial t} \quad (C.10)$$

where the heat capacity per unit area of the tissue  $C_w = C_t w_t/2$ ,  $\Delta H = 2.5 \cdot 10^6 \text{ J}/\text{kg}$  is the latent heat,  $\rho_w$  the evaporated water mass per unit area and the heat capacity  $C_t$  is the heat capacity per unit volume of the tissue. Using the values taken from (Popovic and Minceva, 2020) the heat capacity per volume  $C_t = 3.48 \text{ MJ}/(\text{Km}^3)$ .

We will be taking the evaporation rate to be proportional to the heat per unit area  $q$ , that is  $\Delta H \partial \rho_w / \partial t = \alpha q$ , where  $\alpha$  is a dimensionless constant, which we may determine as follows. Integrating equation (C.10) over the length of the channel and the time of inhalation,

$$\int_0^{t_{br}} dt \int_0^{L_0} dx C_t \frac{\partial T_w}{\partial t} = \int_0^{t_{br}} dt \int_0^{L_0} dx \frac{6\kappa}{w} \Delta \bar{T} + \int_0^{t_{br}} dt \int_0^{L_0} dx \Delta H \frac{\partial \rho_w}{\partial t} \quad (C.11)$$

gives

$$E_{tot} = C_a(T_b - T_a) + \Delta H m_w \quad (C.12)$$

where  $E_{tot}$  is the total energy given off by the tissue, and we have used the fact that the integrated heat that goes into the air must equal the energy  $C_a(T_b - T_a)$  needed to raise its temperature to body temperature. Since, by assumption

$$\Delta H m_w = \alpha C_a(T_b - T_a), \quad (C.13)$$

we may calculate  $\alpha = \Delta H \Delta m / (C_a(T_b - T_a)) \approx 2.2$  (3.9) for Eb (Mm) from the  $m_w$  value of equation (A.4). This yields

$$(1 + \alpha) \frac{6\kappa}{w} \Delta \bar{T} = C_t \frac{\partial T_w}{\partial t}, \quad (C.14)$$

or

$$\frac{\partial T_w}{\partial t} = \frac{\Delta \bar{T}}{\tau_0} = \frac{\bar{T} - T_w}{\tau_0} \quad (C.15)$$

where the time is given by

$$\tau_0 = \frac{C_t w w_t}{12(1 + \alpha)\kappa}. \quad (C.16)$$

### Appendix C.3. Contribution of blood flow

The energy is supplied to the MT by arterial blood which enters the turbinate at a temperature  $T_b$ . Based on anatomical considerations (Folkow et al., 1988), we assume that it enters at the posterior part of the channel walls and flows along the channel, gradually cooling as it gives off heat to the surrounding tissue.

The small distance  $d$  of the arterioles within the turbinate mucosa to the respired airstream ( $d \sim 100 \mu\text{m}$ ) means that there is rapid thermal exchange between the blood and the surrounding tissue. The thermal diffusion time that is required for the blood to give off its heat to the surrounding tissue is  $t_{diff} = d^2/(2D) \approx 0.03 \text{ s}$ , where  $D_w = 1.5 \cdot 10^{-7} \text{ m}^2/\text{s}$  is the thermal diffusivity in water. This time is about 1/30 of the inhalation time, so that on this time scale the internal thermal relaxation in the tissue and blood stream may be considered instantaneous. This means that any given volume of arterial blood that is moving with a velocity  $v_b$  (defined as the volume flux through the arterioles divided by its cross-sectional area) equilibrates almost instantly with the surrounding tissue. At any position  $x$  along the channel the blood and the tissue will therefore have the same temperature. Since equation (C.14) equates the energy flux from the air and the rate at which thermal energy of the tissue changes, we must now add the energy supplied by the blood:

$$(1 + \alpha) \frac{6\kappa}{w} \Delta \bar{T} + c_b \frac{\Delta V_b \Delta T_b}{\Delta A_w \Delta t} = C_w \frac{\partial T_w}{\partial t}, \quad (C.17)$$

where  $c_b$  is the blood heat capacity per volume,  $\Delta V_b = \Delta A_b \Delta x$  is the amount of blood supplied to an element of the channel wall of length  $\Delta x$ , and  $\Delta A_b$  the cross-sectional area of the tissue,  $\Delta T_b$  is the change in blood temperature over this length,  $\Delta A_w$  is an element of the surface area of the wall, and the

limit of the time  $\Delta t \rightarrow 0$  is implied. The blood volume  $\Delta V_b = f\Delta A_b v_b \Delta t$  where  $f$  is the ratio of arterial blood volume to the volume of the bone and soft tissue (arterial fraction), and  $v_b$  is the arterial blood velocity. The ratio of the two surface elements is  $\Delta A_b/\Delta A_w = w_t/\Delta x$ . Taking the blood to have the same heat capacity as the tissue  $c_b = C_w/w_b$ , since the former is a heat capacity per unit volume and the latter per unit area. Given the thermal equilibrium between blood and wall, the change in blood temperature over a length  $\Delta x$  is  $\Delta T_b = \partial T_w/\partial x \Delta x$ . Using these relations in equation (C.17) gives

$$(1 + \alpha) \frac{6\kappa}{w} \frac{\Delta \bar{T}}{\Delta T} + C_w f v_b \frac{\partial T_w}{\partial x} = C_w \frac{\partial T_w}{\partial t}, \quad (\text{C.18})$$

and so, equation (C.15) becomes

$$\frac{\partial T_w}{\partial t} = \frac{\Delta \bar{T}}{\tau_0} = \frac{\bar{T} - T_w}{\tau_0} + f v_b \frac{\partial T_w}{\partial x}, \quad (\text{C.19})$$

which is just Eq. (5) with

$$v = f v_b. \quad (\text{C.20})$$

The  $v$ -term now appears as a positive source term when  $T_w$  increases towards the posterior part of the turbinate, thus representing the heating from the blood.

#### Appendix C.4. Numerical integration of temperature profiles

Starting with the initial condition

$$T_w(x, 0) = T_b \quad (\text{C.21})$$

we solve the temperature problem numerically in the following manner. First, equation (C.7) is multiplied by  $e^{x/l}$ , so that it may be written in the form

$$\frac{\partial}{\partial x} (\bar{T} e^{x/l}) = \bar{T}_w e^{x/l}. \quad (\text{C.22})$$

Integrating this equation from  $x = 0$  to  $x$ , using the boundary condition that  $\bar{T}(0, t) = T_a$  during inhalation, gives

$$\bar{T}(x, t) = T_a e^{-x/l} + \frac{1}{l} \int_0^x dx' e^{-(x-x')/l} T_w(x', t), \quad (\text{C.23})$$

which is easily integrated at each time-step by means of the trapezoidal rule. In a similar way, during expiration when the boundary condition is  $\bar{T}(L_0, t) = T_b$ , equation (C.8) yields

$$\bar{T}(x, t) = \bar{T}_b e^{-(L_0-x)/l} + \frac{1}{l} \int_x^{L_0} dx' e^{-(x'-x)/l} T_w(x', t). \quad (\text{C.24})$$

Next, equation (C.19) is stepped forward in time by means of the simple discretization

$$T_w(x, t + dt) = T_w(x, t) + \left( \frac{\bar{T} - T_w}{\tau_0} + v \frac{\partial T_w}{\partial x} \right) dt, \quad (\text{C.25})$$

for each of 200–400 equally spaced  $x$ -values. The  $x$ -derivative is evaluated by a finite difference, using the first order upwind scheme.

$$\frac{\partial T_w}{\partial x} = \frac{T_w(x + \Delta x) - T_w(x)}{\Delta x}, \quad (\text{C.26})$$

which is stable as long as  $v dt/\Delta x < 1$ .

## References

- Aylward, G., Findlay, T., 2002. *SI Chemical Data*, fifth ed. Wiley.
- Batchelor, G.K., 1967. *An Introduction to Fluid Dynamics*. Cambridge University Press, Cambridge.
- Blix, A., Johnsen, H., 1983. Aspects of nasal heat exchange in resting reindeer. *J. Physiol. Lond.* 340, 445–454.
- Burns, J., 1981. Bearded seal - *Erignathus barbatus*. In: Ridgway, S.H., Harrison, R.J. (Eds.), *Handbook of Marine Mammals*, vol. 6. Academic Press, London, pp. 145–170, 2: Seals.
- Castellini, M., 1996. Dreaming about diving: sleep apnea in seals. *News Physiol. Sci.* 11, 208–213.
- Engineering toolbox Air-thermal diffusivity. Available at: [www.engineeringtoolbox.com](http://www.engineeringtoolbox.com). (Accessed 23 September 2020).
- Favilla, A., Costa, D.P., 2020. Thermoregulatory strategies of diving air-breathing marine vertebrates: a review. *Front. Ecol. Evol.* 8.
- Folkow, L., Blix, A., 1987. Nasal heat and water exchange in gray seals. *Am. J. Physiol.* 253, R883–R889.
- Folkow, L., Blix, A., 1989. Thermoregulatory control of expired air temperature in diving harp seals. *Am. J. Physiol.* 257, R306–R310.
- Folkow, L., Blix, A., Eide, T., 1988. Anatomical and functional aspects of the nasal mucosal and ophthalmic retia of phocid seals. *J. Zool., Lond.* 216, 417–436.
- Huntley, A., Costa, D., Rubin, R., 1984. The contribution of nasal countercurrent heat exchange to water balance in the northern elephant seal, *mirounga angustirostris*. *J. Exp. Biol.* 113, 447–454.

- Kenyon, K., 1981. Monk seal - Monachus. In: Ridgway, S.H., Harrison, R.J. (Eds.), *Handbook of Marine Mammals*, vol. 8. Academic Press, London, pp. 195–220, 2: Seals.
- Kleiber, M., 1961. *The Fire of Life*. John Wiley & Sons, Inc, USA.
- Kooyman, G., 1989. *Diverse Divers: Physiology and Behavior*. Springer Verlag.
- Lester, C.W., Costa, D.P., 2006. Water conservation in fasting northern elephant seals (*Mirounga angustirostris*). *J. Exp. Biol.* 209, 4283–4294.
- Magnanelli, E., Wilhelmsen, Ø., Aquarone, M., Folkow, L., Kjelstrup, S., 2017. The nasal geometry of the reindeer gives energy-efficient respiration. *J. Non-Equilib. Thermodyn.* 42, 59–78.
- Mason, M., Wenger, L., Hammer, Ø., Blix, A.S., 2020. Structure and function of respiratory turbinates in phocid seals. *Polar Biol.* 43, 157–173.
- Matsuura, K., 2020. The Climate Data Guide: Global (Land) Precipitation and Temperature: Willmott and Matsuura, University of Delaware, Retrieved from [climatedataguide.ucar.edu/climate-data/global-land-precipitation-and-temperature-willmott-matsuura-university-delaware](https://climatedataguide.ucar.edu/climate-data/global-land-precipitation-and-temperature-willmott-matsuura-university-delaware).
- Matsuura, D., Whittow, G., 1974. Evaporative heat loss in the California sea lion and harbor seal. *Comp. Biochem. Physiol.* 48 A, 9–20.
- Negus, V., 1958. *The Comparative Anatomy and Physiology of the Nose and Paranasal Sinuses*. E. & S. Livingstone.
- Poling, B., Prausnitz, J., O'Connell, J., Reid, R., 2001. *The Properties of Gases and Liquids*, vol. 5. McGraw-Hill, New York.
- Popovic, M., Minceva, M., 2020. Thermodynamic properties of human tissues. *Therm. Sci.* 24 (6B), 4115–4133.
- Reed, J., Chambers, C., Fedak, M., Butler, P., 1994. Gas exchange of captive freely diving grey seals. *J. Exp. Biol.* 191, 1–18.
- Schmidt-Nielsen, K., Hainsworth, F., Murrish, D., 1970. Counter-current heat exchange in the respiratory passages: effect on water and heat balance. *Respir. Physiol.* 9, 263–276.
- Skog, E., Folkow, L., 1994. Nasal heat and water exchange is not an effector mechanism for water balance regulation in grey seals. *Acta Physiol. Scand.* 151, 233–240.
- Solberg, S., Magnanelli, E., Wilhelmsen, Ø., Aquarone, M., Folkow, L., Kjelstrup, S., 2020. Energy efficiency of respiration in mature and newborn reindeer. *J. Comp. Physiol. B.* 190, 509–520.
- Stanfield, C.L., Germann, W., 2008. *Principles of Human Physiology*. Pearson Benjamin Cummings, San Francisco, USA.
- ToolBox, E.** Diffusion coefficients of gases in excess of air. Available at: [www.engineeringtoolbox.com](http://www.engineeringtoolbox.com). (Accessed 23 September 2020).
- van Valkenburgh, B., Curtis, A., Samuels, J., Bird, D., Fulkerson, B., Meachen-Samuels, J., Slater, G., 2011. Aquatic adaptations in the nose of carnivores: evidence from the turbinates. *J. Anat.* 218, 298–310.
- Walker, J., Wells Jr., R., Merrill Jr., E., 1961. Heat and water exchange in the respiratory tract. *Am. J. Med.* 30, 259–267.
- Widdicombe, J., 1997. Microvascular anatomy of the nose. *Allergy* 52, 7–11.